Applied Catalysis B: Environmental 96 (2010) 387–398

Contents lists available at ScienceDirect

Applied Catalysis B: Environmental

journal homepage: www.elsevier.com/locate/apcatb

New approaches to improving catalyst stability over Pt/ceria during ethanol steam reforming: Sn addition and CO_2 co-feeding

Sania M. de Lima [a,1], Adriana M. da Silva [a], Gary Jacobs [b], Burtron H. Davis [b], Lisiane V. Mattos [a,2], Fábio B. Noronha [a,*]

[a] Instituto Nacional de Tecnologia - INT, Av. Venezuela 82, CEP 20081-312, Rio de Janeiro, Brazil
[b] Center for Applied Energy Research, The University of Kentucky, 2540 Research Park Drive, Lexington, KY 40511, USA

ARTICLE INFO

Article history:
Received 13 August 2009
Received in revised form 15 February 2010
Accepted 25 February 2010
Available online 11 March 2010

Keywords:
Hydrogen production
Ethanol steam reforming
Pt–Sn/CeO_2 catalyst
Deactivation mechanism
Carbon formation
CO_2 co-feeding

ABSTRACT

To promote long-term stability of Pt/CeO_2 catalyst for ethanol steam reforming, two approaches were examined. Sn was added to Pt to suppress carbon formation. Although the catalyst with high Sn content exhibited improved stability, acetaldehyde selectivity was prohibitive. DRIFTS experiments revealed that Sn inhibited the ability of Pt to facilitate steam-assisted forward acetate decomposition reaction to carbonate, the precursor to CO_2 formation. However, CO_2 co-feeding was more effective, not only in promoting long-term catalyst stability, but also in maintaining high H_2 selectivity. DRIFTS experiments indicate that the kinetic influence of CO_2 can be explained as a competition with ethanol for adsorption sites, leading to a suppression in the rate of formation of coke precursors.

1. Introduction

Hydrogen production through steam reforming of ethanol (SR) is an attractive technology since ethanol is a renewable raw material obtained from fermentation of various agricultural products (e.g., sugar cane) [1–3]. Although SR has been extensively studied in the literature [1–9], the development of suitable catalysts is still a significant challenge from the standpoint of catalyst deactivation.

Ethanol reactions on transition metal surfaces comprise a complex system, including several reaction intermediates [10,11]. Several reaction pathways may occur, depending on reaction conditions and choice of the catalyst, which in turn lead to the formation of different by-products like CO, acetaldehyde, acetone, ethene, and methane [2,3]. Some of these reactions may lead to coke formation, which can induce catalyst deactivation. The main reactions that may contribute to coke formation are: (i) ethanol dehydration to ethylene, followed by polymerization to coke (reactions (1) and (2)); (ii) the Boudouard reaction (reaction (3)); (iii) the reverse of carbon gasification (reaction (4)) and (iv) CH_4 decomposition (reaction (5)), as detailed below:

$$C_2H_5OH \rightarrow C_2H_4 + H_2O \quad (1)$$

$$C_2H_4 \rightarrow \text{coke} \quad (2)$$

$$2CO \rightarrow CO_2 + C \quad (3)$$

$$CO + H_2 \rightarrow H_2O + C \quad (4)$$

$$CH_4 \rightarrow C + 2H_2 \quad (5)$$

The extent of each reaction depends on the reaction conditions and the nature of the metal and the support. While low reaction temperature favors the formation of carbon through reactions (3) and (4) carbon formation via reaction (5) is the main route at high temperatures.

The formation of carbon is likely the main issue in applying ethanol conversion reactions to produce H_2 for PEM fuel cell applications. Regardless of the metal and the support used, significant deactivation during SR was reported in the open literature over Pt [8,12,13], Pd [8,14], Rh [8,9,15,16], Ru [8,17], Ir [8,18], Co [19–23], and Ni [7,24–26] based catalysts. The types of carbonaceous deposits formed depend on the nature of the metal selected. On Ni- or Co-based catalysts, carbon formed during reaction diffuses through the Ni or Co crystallite, nucleating carbon filaments which grow behind the metal particle, lifting it from the support and altering the catalyst structure [22,26,27]. However, this, carbon formation does not necessarily induce catalyst deactivation.

* Corresponding author. Tel.: +55 21 2123 1177; fax: +55 21 2123 1166.
E-mail address: fabiobel@int.gov.br (F.B. Noronha).
[1] Present address: Universidade Estadual do Oeste do Paraná - Unioeste, Campus de Toledo, Rua da Faculdade, 645, Jd. La Salle, CEP 85903-000, Toledo, Brazil.
[2] Present address: Universidade Federal Fluminense, Rua Passo da Pátria, 156, Niterói, RJ CEP 24210-240, Brazil.

0926-3373/$ – see front matter © 2010 Elsevier B.V. All rights reserved.
doi:10.1016/j.apcatb.2010.02.036

On noble metal-based catalysts, carbon diffusion does not take place and thus carbon may encapsulate the metal particle or cover the support. Roh et al. [15] studied the deactivation and regeneration of $Rh/CeZrO_2$ catalyst during SR and proposed that catalyst deactivation was due to carbonaceous deposition. The catalyst could be completely regenerated and recover its initial activity after treatment under O_2/He mixture above 473 K. Platon et al. [16] suggested that a significant buildup of reaction intermediates over $Rh/CeZrO_2$ during SR, leads to catalyst deactivation. Erdohelyi et al. [8] proposed that the deactivation of supported noble metal catalysts was caused by the accumulation of acetate-like species over the support, which was suggested to inhibit the migration of ethoxy species from the support to the metal particles and thus, its decomposition. Recently, we have studied the deactivation mechanism of $Pt/CeZrO_2$ during SR [12]. The catalyst was found to deactivate at all of the reaction conditions studied. According to the reaction mechanism proposed, ethanol adsorbs dissociatively as ethoxy species, followed by dehydrogenation to acetaldehyde and acetyl species. The dehydrogenated species may oxidize to acetate species, via the addition of support-bound hydroxyl groups. The decomposition reactions of dehydrogenated and acetate species are promoted by the metal–support interface. The unbalance between the rate of the decomposition reaction and the rate of desorption of CH_x species as CH_4 leads to the accumulation of carbon deposits and obstruction of the Pt–support interface, resulting in catalyst deactivation. The loss of the Pt–support interface results in an increasing steady-state coverage of acetate species with respect to time on stream (TOS).

The nature of the support may also strongly affect the product distribution and catalyst stability during SR since it independently exhibits activity for this reaction [1,2]. Acidic supports such as alumina promote the dehydration of ethanol to ethylene, a precursor to coke [7], while redox supports like ceria and ceria-containing mixed oxides improve catalyst stability due to their high oxygen storage capacities [12,15,18,28–30]. Cai et al. [18] proposed that ceria inhibited coke deposition through oxygen transfer from ceria to Ir particles, thereby contributing to carbon removal from Ir particles. Along similar lines, Song and Ozkan [30] suggested that the high oxygen mobility of ceria suppresses carbon deposition and keeps the particle surface clean.

Different strategies have been adopted to minimize carbon deposition. One approach is to increase the steam/ethanol ratio of the feed, which should favor the gasification of carbon with water (Eq. (4)). However, the effectiveness of this strategy depends on the rate of the gasification reaction, which is generally slow [31]. For example, $Rh/CeZrO_2$ catalyst significantly deactivated during SR even at a high steam-to-ethanol molar ratio (H_2O/ethanol = 8.0) [15]. We also studied the effect of the H_2O/ethanol ratio on the performance of a $Pt/CeZrO_2$ catalyst during SR. Increasing H_2O/ethanol ratio from 2.0 to 10.0 decreased the catalyst deactivation rate but not enough to achieve long-term catalyst stability [12]. Another strategy is to add promoters such as alkali or alkali-containing supports, which accelerate the gasification reaction [31]. However, the addition of 0.5 wt.% of potassium to $Rh/CeZrO_2$ catalyst only slightly improved ethanol conversion but the catalyst still underwent significant deactivation. Adding more K (5 wt.%) strongly decreased catalyst activity [15]. Alkali compounds like K may also neutralize the acid sites on alumina, thereby decreasing the formation of ethylene and, in turn, coke formation. Domok et al. [32] suggest that adding K to Pt/Al_2O_3 lowers the stability of the acetate species, thus reducing its poisoning effect. Despite these attempts, there is yet to be developed an effective procedure that prevents or at least significantly inhibits or mitigates carbon formation during ethanol conversion reactions to produce hydrogen.

The aim of this work is to evaluate two different approaches to minimize or prevent carbon formation during SR of ceria-supported Pt catalyst. The first envisions the control of the size of the site ensembles via the addition of a second metal. PtSn and PtRe catalysts have been extensively used in hydrocarbon reforming reactions [33], since coke formation requires a minimum ensemble of metal atoms [31]. Taking into account the geometric effect, the addition of Sn may dilute the metal atoms by alloying and thereby inhibit coke formation.

The second approach is based on the Boudouard reaction (reaction (3)). The addition of CO_2 to the feed may shift the equilibrium in favor of reactants and help to diminish carbon formation. This CO_2 may be recirculated from the outlet stream of the PEM fuel cell.

2. Experimental

2.1. Catalyst preparation

Cerium (IV) ammonium nitrate was calcined in a muffle furnace at 1073 K for 1 h. The ramp rate used was 5 K/min. Pt (1 wt.%) was added to CeO_2 by incipient wetness impregnation using an aqueous solution of H_2PtCl_6, whereas tin (0.6 and 2.6 wt.%) was added using an aqueous solution of $SnCl_2$ (Merck). After impregnation, the samples were dried at 393 K and calcined under flowing air (50 mL/min) at 673 K for 2 h. The following catalysts were obtained: Pt/CeO_2; $PtSn/CeO_2$ (atomic ratio = 1.0); and $PtSn_4/CeO_2$ (atomic ratio = 4.25).

2.2. Temperature-programmed desorption of ethanol (TPD)

TPD experiments of adsorbed ethanol were carried out using a micro-reactor coupled to a quadrupole mass spectrometer (QMS) (Omnistar, Balzers). Prior to TPD analyses, the samples were reduced under flowing H_2 (30 mL/min) by ramping to 773 K (10 K/min), and holding for 1 h. The system was purged with helium at 773 K for 30 min and cooled to room temperature. The adsorption of ethanol was carried out at room temperature using an ethanol/He mixture, which was obtained by flowing He through a saturator containing ethanol at 298 K. After adsorption, the catalyst was heated at 20 K/min to 773 K under flowing helium (60 mL/min). The products were monitored using a QMS.

2.3. Temperature-programmed oxidation (TPO)

TPO was used to characterize the nature and the quantity of carbon formed over Pt/CeO_2 and $PtSn/CeO_2$ catalyst after 6 h of reaction (TOS). The analysis was performed in the same apparatus described previously for TPD measurements. After reaction, the catalyst was cooled to room temperature under He, then heated at a rate of 10 K/min to 1273 K under a mixture containing 8% O_2 in He. The products were monitored using a QMS.

2.4. Diffuse reflectance infrared spectroscopy (DRIFTS)

DRIFTS spectra were recorded using a Nicolet Nexus 870 spectrometer equipped with a DTGS-TEC detector. A Thermo Spectra-Tech cell capable of high pressure/high temperature operation and fitted with ZnSe windows served as the reaction chamber for in situ adsorption and reaction measurements. Scans were taken at a resolution of 4 to give a data spacing of 1.928 cm^{-1}. Depending on the signal-to-noise ratio, the number of scans ranged from 256 to 1024. The amount of catalyst was ~40 mg.

Samples were first reduced in 200 mL/min H_2:He (1:1) at 773 K for 1 h. A temperature ramp of 10 K/min was used. The catalyst was purged in flowing He at 773 K, prior to cooling in flowing He to 313 K.

For ethanol adsorption and SR reaction tests, He was bubbled at ~15 mL/min through a saturator filled with ethanol and held at

273 K. For SR tests, a second helium stream (~15 mL/min) was bubbled through a saturator filled with water and held at 298 K. The two steams were joined at a tee-junction, prior to which 1 psig check valves were placed on the lines to prevent a back-flow condition. The saturator gas flows and temperatures were set to provide a H_2O:CH_3CH_2OH stoichiometric ratio of 2:1.

For CO_2 co-feeding experiments, 15 mL/min was flowed through each saturator and 6 mL/min of 15% CO_2/He was co-fed to adjust the CO_2/CH_3CH_2OH ratio to 4.0.

Adsorption/reaction measurements were started at 313 K, and then the temperature was increased at 10 K/min, pausing at intervals to record spectra at 373, 473, 573, 673 and 773 K. To explore the deactivation of the catalyst, several spectra were recorded during steady-state SR reaction at 773 K over 6 h.

2.5. Reaction conditions

2.5.1. Ethanol hydrogenolysis

The ethanol hydrogenolysis reactions were performed over Pt/CeO_2, $PtSn/CeO_2$ and $PtSn_4/CeO_2$ catalysts, in order to evaluate the effect of Sn addition to the properties of the metallic sites. The catalysts were first reduced at 773 K for 1 h and then purged in N_2 for 30 min (773 K). All reactions were carried out at 773 K, using a H_2/ethanol molar ratio of 9.5 and a residence time (W/Q) of 0.02 g s/mL. The samples were diluted with inert SiC (SiC mass/catalyst mass = 3.0). The reactant mixture was obtained by flowing a H_2 stream through a saturator containing ethanol (30 mL/min) and combining it with a N_2 stream (30 mL/min).

The reaction products were analyzed by gas chromatography (Micro GC Agilent 3000 A) containing two channels for dual thermal conductivity detectors (TCD) and two columns: a molecular sieve and a Poraplot U column. Ethanol conversion and selectivity to products were determined from:

$$X_{ethanol} = \frac{(n_{ethanol})_{fed} - (n_{ethanol})_{exit}}{(n_{ethanol})_{fed}} \times 100 \quad (6)$$

$$S_x = \frac{(n_x)_{produced}}{(n_{total})_{produced}} \times 100 \quad (7)$$

where $(n_x)_{produced}$ is the moles of x produced (x = hydrogen, CO, CO_2, methane, acetaldehyde or ethene) and $(n_{total})_{produced}$ the moles of H_2 + moles of CO + moles of CO_2 + moles of acetaldehyde + moles of ethene (the moles of water produced are not included).

2.5.2. SR

SR was performed in a fixed-bed reactor at atmospheric pressure in the same apparatus used for ethanol hydrogenolysis experiments. Prior to reaction testing, catalysts were reduced at 773 K, for 1 h and then purged with N_2 at 773 K for 30 min. All reactions were carried out at 773 K and two H_2O/ethanol molar ratios (3.0 and 10.0) were utilized. The desired H_2O/ethanol molar ratio was obtained by flowing two N_2 streams (30 mL/min) through saturators containing ethanol and water separately, which were maintained at the required temperature. The partial pressure of ethanol was maintained constant for all experiments. The variation of partial pressure of water was compensated by a decrease in the partial pressure of N_2. Some SR tests were performed in the presence of CO_2, and the reactant mixture was obtained by flowing a N_2 stream through a saturator containing ethanol (30 mL/min) and combining it with a separate CO_2 stream that was flowed through a saturator containing water (30 mL/min), resulting in a CO_2/ethanol molar ratio of 4.0.

In order to observe catalyst deactivation within a short period of time, a small amount of catalyst was used (20 mg diluted with SiC). The reaction products were analyzed by gas chromatography as described previously.

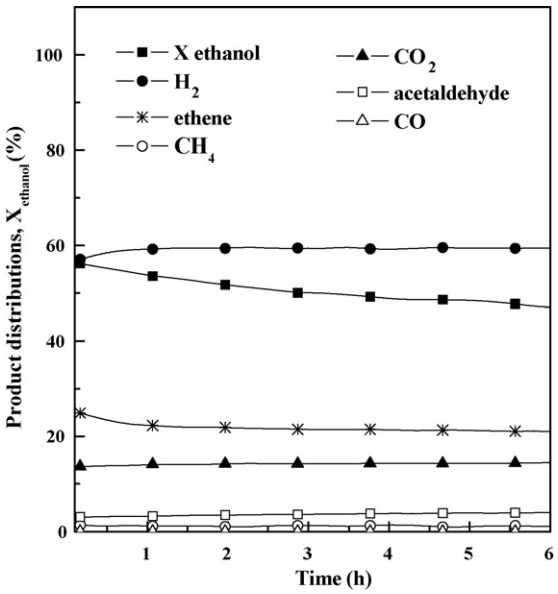

Fig. 1. Ethanol conversion ($X_{ethanol}$) and product distributions versus TOS obtained for SR over CeO_2. *Reaction conditions*: mass of catalyst = 20 mg; H_2O/ethanol molar ratio = 3.0; $T_{reaction}$ = 773 K; residence time = 0.02 g s/mL.

3. Results and discussion

3.1. Reactions

The support plays an important role in the SR of ethanol. Recently, we demonstrated that CeO_2 is a highly active material for the SR of ethanol, producing hydrogen free of CO as well as carbon deposits [34]. Therefore, we decided to investigate the performance of CeO_2 on SR.

3.1.1. SR over CeO_2

The ethanol conversion and product distributions as a function of TOS obtained for CeO_2 during SR (773 K; H_2O/ethanol molar ratio = 3.0) are presented in Fig. 1. The support was very active for SR of ethanol. The initial conversion of ethanol was 55%, declining to a stable conversion of 50% after an initial period of deactivation. Regarding product distributions, hydrogen was the main product obtained (60–70%) while CO_2, acetaldehyde and ethylene were also detected.

3.1.2. SR over Pt/CeO_2

Fig. 2a shows the ethanol conversion and product distributions as a function of TOS obtained for Pt/CeO_2 during SR at 773 K, using a H_2O/ethanol molar ratio of 3.0. The ethanol conversion was quite stable during 3 h TOS, but then significantly deactivated. The decrease in ethanol conversion was accompanied by a decrease in H_2 selectivity and an increase in acetaldehyde selectivity. Besides H_2 and acetaldehyde, small quantities of CO_2 and methane and trace amounts of CO were also observed. No significant formation of ethylene was detected during the reaction. Relative to the support alone, the addition of platinum led to an increase in initial conversion of ethanol, a significant decrease in stability and a reduction in ethylene selectivity.

Increasing the water to ethanol molar ratio to 10 increased the period of stability (5 h TOS), but did not promote long-term catalyst stability (Fig. 2b). Regarding product distributions, the selectivity to H_2 was more stable and the acetaldehyde production was lower at the higher ratio.

We also detected a significant deactivation for $Pt/CeZrO_2$ catalyst during SR using different H_2O/ethanol molar ratios [12]. The

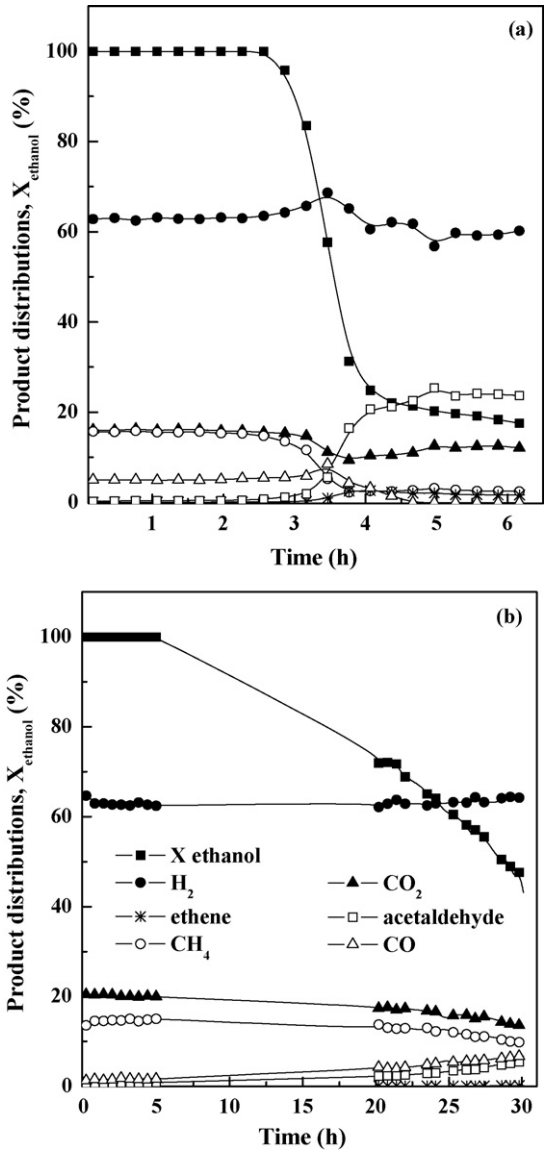

Fig. 2. Ethanol conversion ($X_{ethanol}$) and product distributions versus TOS obtained for SR over Pt/CeO_2 (a) H_2O/ethanol molar ratio = 3.0; (b) H_2O/ethanol molar ratio = 10.0. *Reaction conditions*: mass of catalyst = 20 mg; $T_{reaction}$ = 773 K; residence time = 0.02 g s/mL.

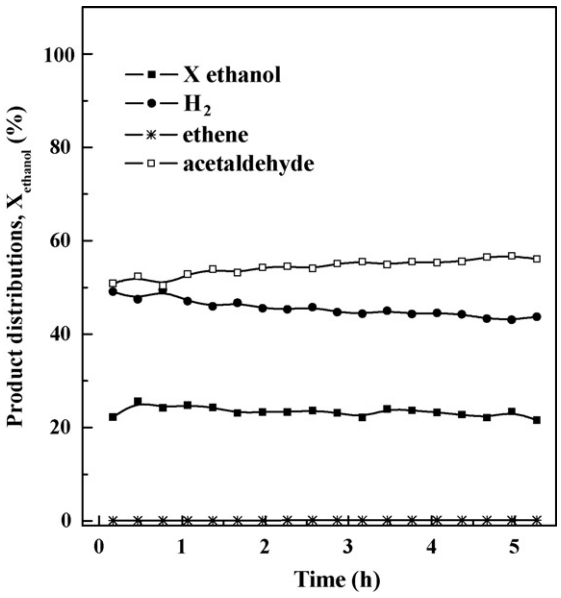

Fig. 3. Ethanol conversion ($X_{ethanol}$) and product distributions versus TOS obtained for SR over SnO_2. *Reaction conditions*: mass of catalyst = 20 mg; $T_{reaction}$ = 773 K; H_2O/ethanol molar ratio = 3.0; residence time = 0.02 g s/mL.

addition of platinum to $CeZrO_2$ support significantly decreased the stability of the catalyst during SR at 773 K [12]. DRIFTS, transmission electron microscopy and TPO and TPD showed that the deactivation of $Pt/CeZrO_2$ catalyst is likely due to the deposition of carbonaceous residue, which leads to the loss of the Pt–support synergy [12]. According to the mechanism proposed, the presence of the metal and water promoted the decomposition of dehydrogenated and acetate species, which occurs at the Pt–support interface. Once the interfacial boundary is lost, the demethanation of acetate becomes hindered, resulting in an increase in acetaldehyde selectivity with TOS. For $Pt/CeZrO_2$ catalyst, the rate of acetate species decomposition to CH_x, CO and CO_2 should be higher than the rate of desorption of CH_x species as CH_4. The CH_x species formed may lead to the blockage of Pt–support interface resulting in catalyst deactivation. In the case of the $CeZrO_2$ support, the results suggest that there is a proper balance between the rate of acetate decomposition and the rate of desorption of CH_x species which may promote catalyst stability.

Then, in this work, the strong deactivation of ceria-supported platinum catalysts is likely associated with the deposition of carbonaceous residue during the reaction. On the other hand, the stability of the supports could be attributed to a proper balance between the rate of acetate decomposition and the rate of CH_x species desorption.

In addition, even if there is a blockage of the Pt–support interface due to the accumulation of CH_x species, ethanol conversion should remain around 50%, since this is the steady-state conversion level obtained for CeO_2 during the reaction. However, the ethanol conversion was 20% after 6 h TOS over Pt/CeO_2. An ethanol conversion level of 20% corresponds that of the homogeneous reaction (i.e., without catalyst). This suggests that the carbon formed not only covered the Pt–oxide surface, but also the support surface. We also reported similar findings for SR at 773 K in comparing results between the $CeZrO_2$ support and the $Pt/CeZrO_2$ catalyst [12].

Thus, there is an important tradeoff by adding Pt to ceria – while the initial H_2 yield increases significantly, the stability is adversely impacted due to carbon deposition. With the aim of avoiding carbon formation during SR over Pt/CeO_2, two different approaches were evaluated: (i) addition of a second metal (Sn) and (ii) addition of CO_2 to the feed.

3.1.3. The impact of Sn addition to the Pt/CeO_2 catalyst on SR

SR was carried out at 773 K with a H_2O/ethanol molar ratio of 3.0 over SnO_2 (Fig. 3) with the aim of studying the activity of the tin oxide for this reaction. Although SnO_2 was stable during the reaction, it exhibited low ethanol conversion (~25%), close to the conversion of the homogeneous reaction. Hydrogen (~45%) and acetaldehyde (~55%) were the only products detected.

Fig. 4a and b display the ethanol conversion and product distributions as a function of TOS obtained for $PtSn/CeO_2$ and $PtSn_4/CeO_2$ catalysts during SR at 773 K, using a H_2O/ethanol molar ratio of 3.0. Initial ethanol conversion was complete for $PtSn/CeO_2$ and $PtSn_4/CeO_2$ catalysts. At the beginning of the reaction, $PtSn/CeO_2$ catalyst remained stable. After that, the catalyst exhibited a deactivation trend, which was less significant than that observed for the Pt/CeO_2 catalyst (Fig. 2a). The ethanol conversion decreased from 100 to 20 and 65% on Pt/CeO_2 and $PtSn/CeO_2$, respectively, during 6 h TOS. On the other hand, only a slight decrease in the activity was observed for $PtSn_4/CeO_2$ catalyst after 30 h TOS. Despite high selectivity to H_2, the formation of the acetaldehyde was sig-

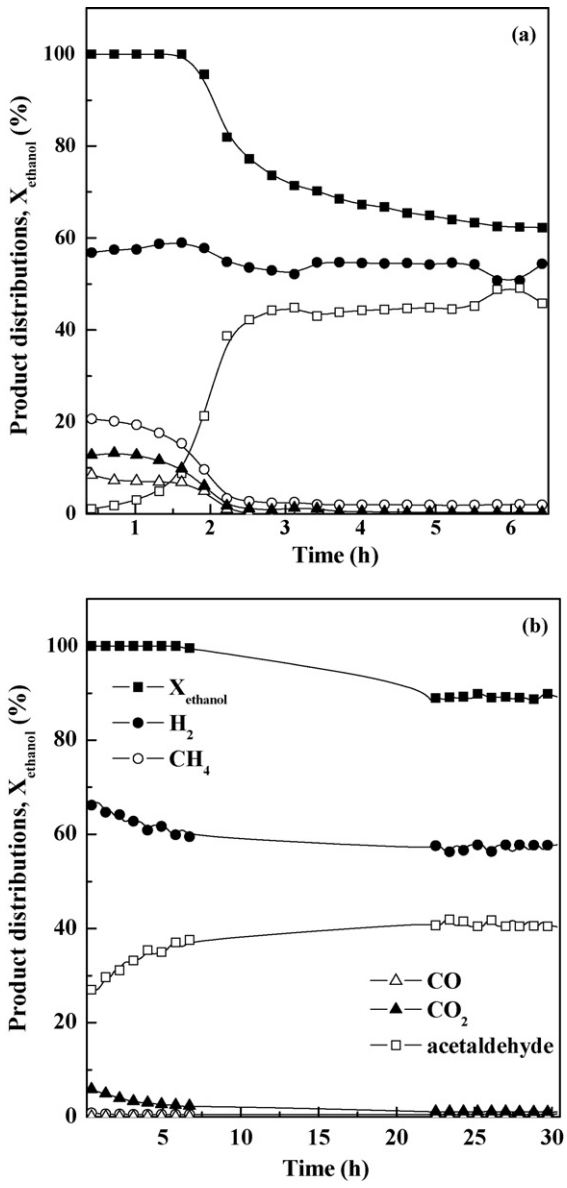

Fig. 4. Ethanol conversion ($X_{ethanol}$) and product distributions versus TOS obtained for SR over (a) $PtSn/CeO_2$ and (b) $PtSn_4/CeO_2$. *Reaction conditions*: mass of catalyst = 20 mg; $T_{reaction}$ = 773 K; H_2O/ethanol molar ratio = 3.0; residence time = 0.02 g s/mL.

nificantly higher for the PtSn catalysts. As observed for Pt/CeO_2, the decrease in ethanol conversion was followed by a decrease in H_2 production and an increase in acetaldehyde formation over the samples containing Sn. In addition to H_2 and acetaldehyde, all samples exhibited CH_4 and CO_2 formation, which were lower for the $PtSn_4/CeO_2$ catalyst. Moreover, small amounts of CO were also detected over the $PtSn/CeO_2$ catalyst. Ethene production was not significant for either PtSn catalyst. It is clear that the addition of tin improved the stability of the catalysts, but also increased the selectivity to acetaldehyde and decreased the selectivities toward CO and CH_4. These results suggest that Sn addition suppressed carbon formation by inhibiting the decomposition of intermediates, resulting in desorption of acetaldehyde.

Alcala et al. [35] reported similar results when they studied the kinetics of the ethanol conversion in the presence of hydrogen over Pt/SiO_2 and $PtSn/SiO_2$ (0.8 or 4.4 wt.% of Sn). The main products formed over Pt/SiO_2 were CH_4, CO, acetaldehyde and ethane. The addition of Sn led to a decrease in CH_4, CO and ethane formation and an increase in acetaldehyde production. According to the authors, the acetaldehyde is initially produced by ethanol dehydrogenation. The acetaldehyde can decompose to CO and CH_4 through the cleaving of the C–C bond. The cleavage of C–O bond of the carbonyl group from the acetaldehyde produces ethane. The rates of the C–C and C–O bond breaking reactions in dehydrogenated species were lower for the catalysts containing tin. The results from in situ ^{119}Sn Mössbauer spectroscopy and CO adsorption microcalorimetry showed that the Pt–Sn alloy is the active phase for the $PtSn/SiO_2$ catalyst. The hydrogenation–dehydrogenation reactions are favored over Pt–Sn alloy, whereas the decomposition reactions are promoted by Pt.

Table 1
Product distributions obtained for ethanol hydrogenolysis over Pt/CeO_2, $PtSn/CeO_2$ and $PtSn_4/CeO_2$ catalysts ($T_{reaction}$ = 773 K; H_2/ethanol = 12.0; W/Q = 0.02 g s/mL).

Catalyst	CH_4	CO	CO_2	Acetaldehyde	Ethene
Pt/CeO_2	74	23	3	0	0
$PtSn/CeO_2$	49	48	1.8	0	1.3
$PtSn_4/CeO_2$	27	28	18	25	2

3.1.4. Ethanol hydrogenolysis

In order to evaluate the effect of Sn addition on the properties of metallic sites, the ethanol hydrogenolysis reaction was performed over Pt/CeO_2, $PtSn/CeO_2$ and $PtSn_4/CeO_2$ catalysts at 773 K.

Ethanol conversion was complete for all the catalysts studied. The product distributions obtained are presented in Table 1. CH_4 and CO were the main products detected over Pt/CeO_2 and $PtSn/CeO_2$ catalysts. In the case of $PtSn_4/CeO_2$, besides CH_4 and CO formation, significant amounts of acetaldehyde and CO_2 were also produced. In addition, trace amounts of ethylene were detected for the PtSn catalysts.

Taking into account the stoichiometry of the ethanol decomposition reaction (Eq. (8)), equimolar amounts of CH_4 and CO should be produced during this reaction, as observed for $PtSn/CeO_2$ and $PtSn_4/CeO_2$ catalysts. However, the CH_4/CO molar ratio was approximately 3.0 over Pt/CeO_2 catalyst. This result could be explained by the occurrence of two parallel reactions during ethanol hydrogenolysis (Eqs. (8) and (9)). The production of CH_4 and water through the reaction between ethanol and hydrogen (Eq. (9)) should be favored over the Pt/CeO_2 catalyst, which leads to a CH_4/CO molar ratio of 3.0, as shown by the global reaction (Eq. (10)).

$$CH_3CH_2OH \rightarrow CH_4 + CO + H_2 \quad (8)$$

$$CH_3CH_2OH + 2H_2 \rightarrow 2CH_4 + H_2O \quad (9)$$

$$2CH_3CH_2OH + H_2 \rightarrow 3CH_4 + CO + H_2O \quad (10)$$

Moreover, the results revealed that the addition of Sn decreased CH_4 production and increased acetaldehyde formation, suggesting that ethanol hydrogenolysis was inhibited and ethanol dehydrogenation was favored with the presence of tin. Since the hydrogenolysis reaction is a structure sensitive reaction [36], it is clear that there is a Pt–Sn interaction on $PtSn/CeO_2$ and $PtSn_4/CeO_2$ catalysts. These results are in agreement with those reported by Alcala et al. [35] and confirm that Sn addition inhibits C–C and C–O bond breaking reactions during SR over the catalysts studied in the present work.

To probe the effect of Sn addition to Pt/CeO_2 catalyst from the standpoint of the SR mechanism, TPD and DRIFTS were employed.

3.2. Reaction mechanism

3.2.1. TPD of ethanol

The TPD profiles of ethanol obtained for Pt/CeO_2, $PtSn/CeO_2$ and $PtSn_4/CeO_2$ catalysts are presented in Fig. 5a–c.

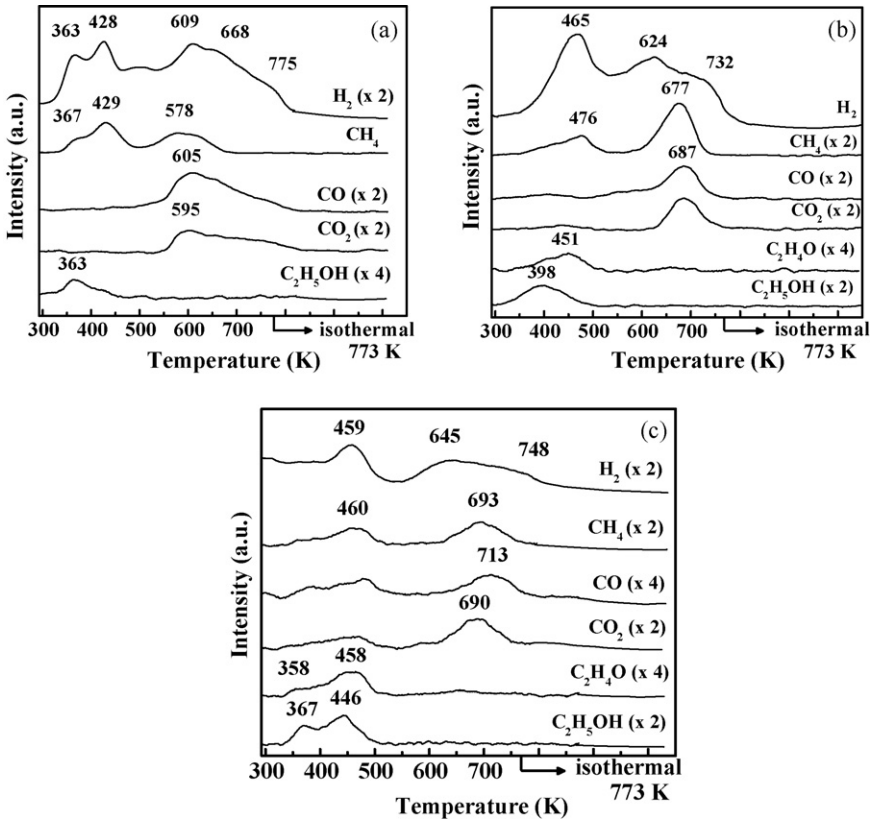

Fig. 5. TPD of adsorbed ethanol profiles for (a) Pt/CeO_2; (b) $PtSn/CeO_2$ and (c) $PtSn_4/CeO_2$. Temperature ramp: 20 K/min; He flow rate = 60 mL/min.

Ethanol desorption was detected at 363 and 398 K for Pt/CeO_2 and $PtSn/CeO_2$, respectively. Similar results have been reported for supported Pt catalysts [12,37]. In the case of the catalyst with higher Sn loading, two peaks corresponding to molecular ethanol desorption were observed at 367 and 446 K. These results suggest that the peaks around 360 and 446 K may be related to ethanol adsorption on Pt and tin oxides, respectively.

At low temperatures, all catalysts exhibited significant formation of H_2 between 350 and 500 K (Pt/CeO_2: 363 and 428 K; $PtSn/CeO_2$: 465 K; $PtSn_4/CeO_2$: 459 K). The production of H_2 was followed by CH_4 formation for all catalysts studied (Pt/CeO_2: 367 and 429 K; $PtSn/CeO_2$: 476 K; $PtSn_4/CeO_2$: 460 K). Pt/CeO_2 catalyst presented the highest level of CH_4 formation. Moreover, the production of H_2 and CH_4 was detected at lower temperatures over Pt/CeO_2 catalyst and CO was not significantly observed for all samples. de Lima et al. [12] also reported the formation of H_2 and CH_4 in the low-temperature region during TPD of ethanol over $CeZrO_2$ supported Pt catalyst. In that investigation, the ethanol was observed to adsorb on the catalyst surface as ethoxy species that could subsequently decompose to H_2, CH_4 and CO with the aid of the metal particles. CO still remained adsorbed on the metal surface and was not detected at low temperatures. Acetaldehyde, which was formed by the dehydrogenation of ethoxy species [12,37], was only observed over $PtSn/CeO_2$ (451 K) and $PtSn_4/CeO_2$ catalysts (358 and 458 K).

At high temperatures, all catalysts exhibited the simultaneous formation of methane (Pt/CeO_2: 578 K; $PtSn/CeO_2$: 677 K; $PtSn_4/CeO_2$: 693 K), CO (Pt/CeO_2: 605 K; $PtSn/CeO_2$: 687 K; $PtSn_4/CeO_2$: 713 K) and CO_2 (Pt/CeO_2: 595 K; $PtSn/CeO_2$: 687 K; $PtSn_4/CeO_2$: 690 K). In addition, the production of methane and CO was lower for the $PtSn_4/CeO_2$ catalyst. No significant levels of crotonaldehyde, acetone or benzene were observed for all catalysts studied. Peaks for CO and methane in the high temperature region during TPD over CeO_2-based catalysts are associated with the decomposition of dehydrogenated and acetate species previously formed [12,37]. The acetate species are produced through the reaction of dehydrogenated species with the surface OH groups and/or oxygen from the support. A fraction of the acetate species can be oxidized to carbonate species, which may in turn be further decomposed to CO_2. The lower peak intensities for methane and CO formation detected over $PtSn_4/CeO_2$ indicate that the decomposition of dehydrogenated and acetate species is not favored in the presence of Sn, in agreement with the results obtained during SR and ethanol hydrogenolysis. The production of H_2 at high temperature in the TPD profiles of all catalysts could be assigned to desorption of H_2 previously formed during the different steps of ethanol dehydrogenation.

3.2.2. DRIFTS analysis at different temperatures under a mixture ethanol + water

Fig. 6 shows the DRIFTS spectra of Pt/CeO_2 under the reaction mixture containing ethanol and water obtained at different temperatures. By comparison with previous reports of the analog methoxy species [38], the bands at 1049 and 1082 cm^{-1} in the spectrum at room temperature correspond to ν(OC) stretching modes of Type II ethoxy species, which were formed by dissociative adsorption of ethanol over Ce^{3+} atoms on the surface of ceria. This is consistent with a reduced surface shell, since H_2 treatment generates defect-associated Type II bridging OH groups which are displaced by ethoxy species [29,38].

Besides the bands related to ethoxy species, the DRIFTS spectrum of Pt/CeO_2 obtained at room temperature exhibited bands at 1456 and 1558 cm^{-1}, which are assigned to ν_s(OCO) and ν_a(OCO) vibrational modes of acetate species, respectively. The bands at 2899, 2931 and 2978 cm^{-1} are also associated with the different vibrational modes (e.g., C–H stretching) of ethoxy and

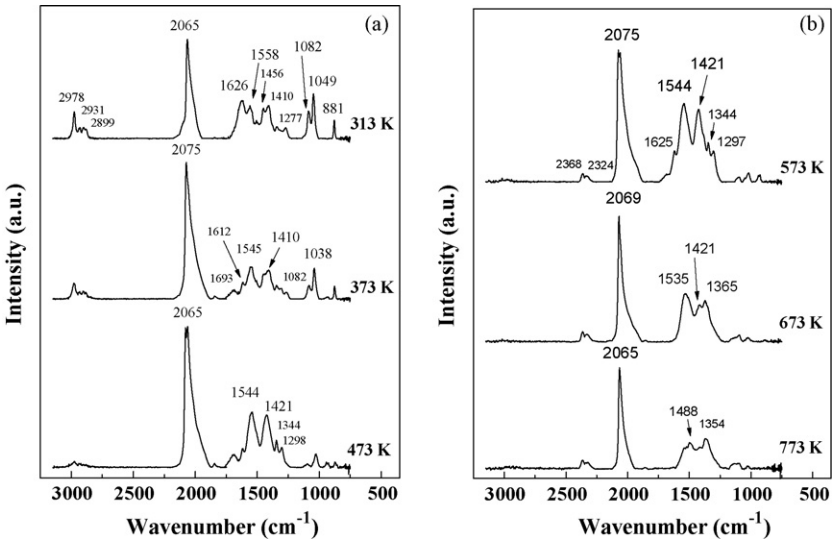

Fig. 6. DRIFTS spectra obtained on Pt/CeO_2 catalyst at different temperatures and under the reaction mixture containing ethanol and water (water/ethanol ratio = 2.0).

acetate species [11]. The presence of the bands assigned to acetate species indicates that ethoxy species were further oxidized to acetate species. Acetate species can be formed by two different routes [8]. At first, ethoxy species are dehydrogenated to acetaldehyde, followed by dehydrogenation to acetyl species. The acetyl species may react with the oxygen from the support producing acetate species. The second reaction pathway involves the reaction between acetaldehyde and surface OH groups from the support. In the present work, the density of O* adatoms available for reaction should be low, since the surface of the catalyst has been partially reduced by the hydrogen treatment. Therefore, the route comprising the reaction between ethoxy species and hydroxyl groups from the support may be favored, as previously suggested for $Pt/CeZrO_2$ [12].

In addition to the bands assigned to ethoxy and acetate species, the spectrum of Pt/CeO_2 exhibited a band attributed to the ν(CO) mode of linearly adsorbed CO on small Pt particles (2065 cm^{-1}) [12,29]. A band at around 1626 cm^{-1} may correspond to acetyl species [12,29], but any assignment is complicated by the bending mode of adsorbed water.

At 373 K, the intensity of the bands corresponding to ethoxy species decreased whereas the intensity of the bands assigned to CO adsorbed on metal particles increased. Furthermore, a shoulder at 1938 cm^{-1} was detected, corresponding to the ν(CO) mode of bridge-bonded CO associated with large Pt particles. On the other hand, the bands related to acetate species remained unchanged. The decrease in the intensities of bands corresponding to ethoxy species and the increase of those associated with CO formation is in accordance with ethanol decomposition to CO, methane and hydrogen. A weak band observed in the spectrum at around 1693 cm^{-1} may be assigned to acetaldehyde species [12,13,29].

When the Pt/CeO_2 catalyst was heated to 473 K, the bands associated with ethoxy species were no longer detected whereas the intensities of the bands attributed to acetate species slightly increased. In addition, the intensity of the band corresponding to CO (2065 cm^{-1}) remained unchanged. These results are consistent with the TPD of adsorbed ethanol (Fig. 5a), which revealed desorption of CH_4 and hydrogen between 418 and 469 K. The increase of the CO band and the corresponding decrease of the bands for ethoxy species confirm that the decomposition of ethoxy species

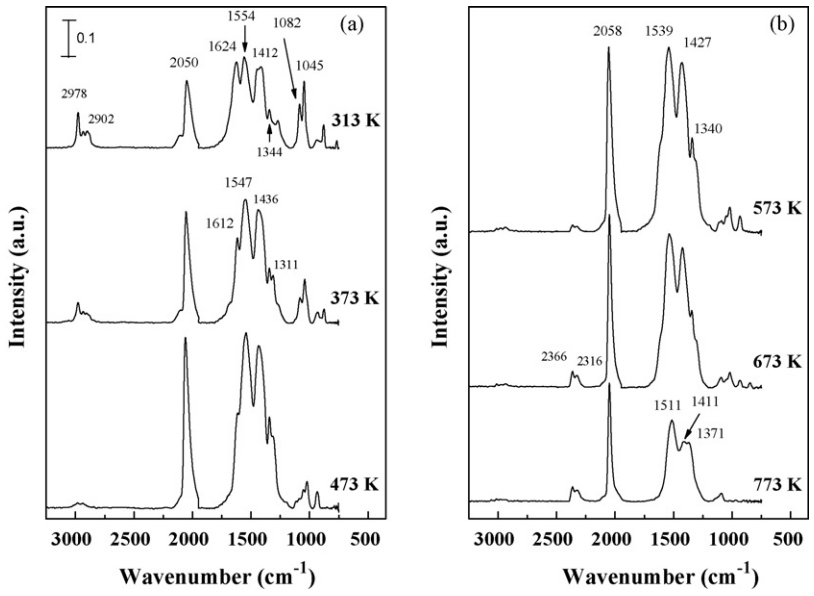

Fig. 7. DRIFTS spectra obtained on $PtSn/CeO_2$ catalyst at different temperatures and under the reaction mixture containing ethanol and water (water/ethanol ratio = 2.0).

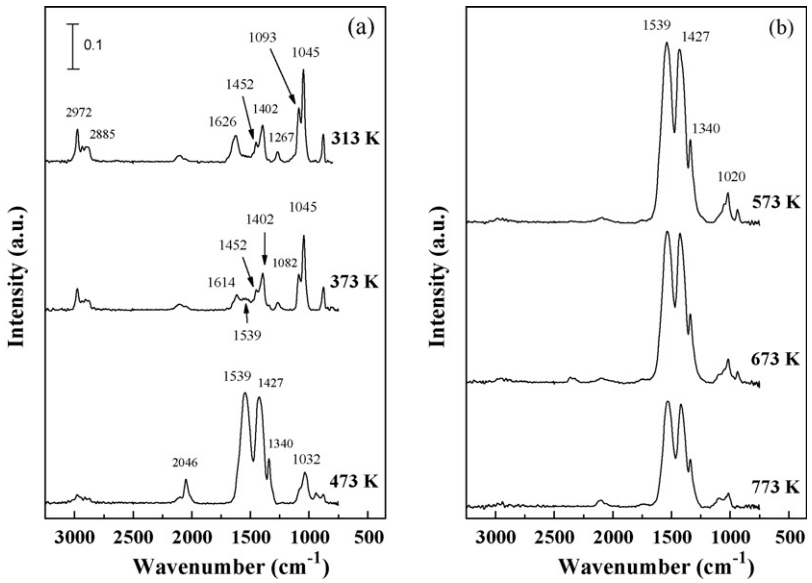

Fig. 8. DRIFTS spectra obtained on $PtSn_4/CeO_2$ catalyst at different temperatures and under the reaction mixture containing ethanol and water (water/ethanol ratio = 2.0).

occurs in the low-temperature region and that CO formed remained adsorbed on the Pt component of the catalyst. de Lima et al. [12] reported similar results during DRIFTS of ethanol desorption over $Pt/CeZrO_2$ catalyst. Domok et al. [13] also detected the formation of hydrogen and methane during combined IR/MS experiments, indicating that decomposition of both ethoxy and acetaldehyde species contributes to the formation of CH_4, hydrogen and CO.

Increasing temperature to 573 K resulted in an increase in the intensity of bands related to acetate species and a decrease in the intensity of the band corresponding to acetaldehyde. The intensity of the CO band remained unchanged and gas phase CO_2 was clearly present (~2350 cm^{-1}). Above 573 K, the intensities of bands characteristic of acetate species and adsorbed CO on Pt decreased. In addition, the presence of carbonate species should be considered, since the bands in the range of 2889–2978 cm^{-1} (i.e., corresponding to C–H stretching modes) were no longer detected.

The DRIFTS spectra of $PtSn/CeO_2$ catalyst under the reaction mixture containing ethanol and water obtained at different temperatures are presented in Fig. 7. At room temperature, the spectrum exhibited the same bands observed during DRIFTS analysis of Pt/CeO_2 (Fig. 6): (i) 1045, 1082 and 1412 cm^{-1} (ν(CO) and δ_{as} (CH_3) modes of ethoxy species); (ii) 1344 and 1554 cm^{-1} (δ_s (CH_3) and ν_{as} (OCO) modes of acetate species); (iii) 2050 cm^{-1} (CO linearly adsorbed); (iv) 1626 cm^{-1} (ν(CO) of acetyl species); and (v) 2902 and 2978 cm^{-1} (C–H vibrations in the ethoxy and acetate species).

Heating the catalyst to 473 K resulted in a significant decrease in the bands corresponding to ethoxy and acetyl species and an increase in the bands related to acetate species and adsorbed CO.

After the sample was heated to 673 K, the ethoxy and acetyl species were no longer detected and the absence of the bands around 2970–2880 cm^{-1} (i.e., corresponding to C–H stretching modes) suggests that carbonate species was formed. Moreover, the bands assigned to gas phase CO_2 (~2350 cm^{-1}) appeared. As observed in TPD analysis, the acetate species undergo steam-assisted forward decomposition to CH_4 and CO or CO_2 via carbonate species at high temperatures. Increasing the temperature to 773 K decreased the bands of adsorbed CO and the bands associated with acetate/carbonate species.

Fig. 8 shows the DRIFTS spectra of $PtSn_4/CeO_2$ under the reaction mixture (ethanol and water) obtained at different temperatures. At room temperature, only bands corresponding to ethoxy (1045, 1093, 1402 and 1452 cm^{-1}) and acetyl species (1626 cm^{-1}) were observed. No bands assigned to acetate species were detected at this temperature. It is remarkable that the bands attributed to adsorbed CO are virtually absent from the spectrum.

The spectrum at 373 K reveals that the intensities of the bands corresponding to ethoxy (1045 and 1093 cm^{-1}) and acetyl species (1626 cm^{-1}) diminished but the bands characteristic of acetate species did not appear.

When the sample was heated to 473 K, the bands related to ethoxy and acetyl species disappeared. Moreover, the bands at 1300–1600 cm^{-1} increased and the bands around 2970–2880 cm^{-1} were no longer detected. This result suggests that this sample contains mainly carbonate species at 473 K. In addition, the band assigned to adsorbed CO was only detected at 473 K. A further increase in temperature to 573 K led to an increase in the intensities of carbonate bands. Increasing temperature to 773 K resulted in a decrease in the intensities of carbonate bands.

A comparison between the DRIFTS spectra obtained for all catalysts (Figs. 6–8) shows that the intensity of the bands assigned to carbonate species are much higher on the samples containing tin. It was also observed that the formation of CO was much lower over $PtSn_4/CeO_2$. In addition, there are significant differences in the relative intensities of the bands corresponding to each species. At room temperature, the ratio between the intensity of bands associated with adsorbed CO and ethoxy species (adsorbed CO/ethoxy ratio) decreased in the order $Pt/CeO_2 > PtSn/CeO_2 > PtSn_4/CeO_2$, which suggests that the decomposition of ethoxy species to H_2, CH_4 and CO is not favored on the samples containing tin. At high temperatures, the Pt/CeO_2 catalyst exhibited the highest adsorbed CO/acetate ratio ($Pt/CeO_2 > PtSn/CeO_2 > PtSn_4/CeO_2$), indicating that the decomposition of acetate species is not facilitated by tin addition. These results confirm that the Pt–support interface is blocked by tin, which inhibits the promotional effect of Pt on the steam-assisted forward acetate decomposition during demethanation as previously described for $Pt/CeZrO_2$ [12]. That is, the steady-state coverage of the acetate over Pt/ceria is lower, because of its higher turnover frequency relative to the Sn-doped samples.

Therefore, the carbon species desorb as acetaldehyde or remain adsorbed as carbonate species over $PtSn/CeO_2$ and $PtSn_4/CeO_2$ catalysts. This result can explain the higher selectivity to acetaldehyde and the lower selectivities to CO and CH_4

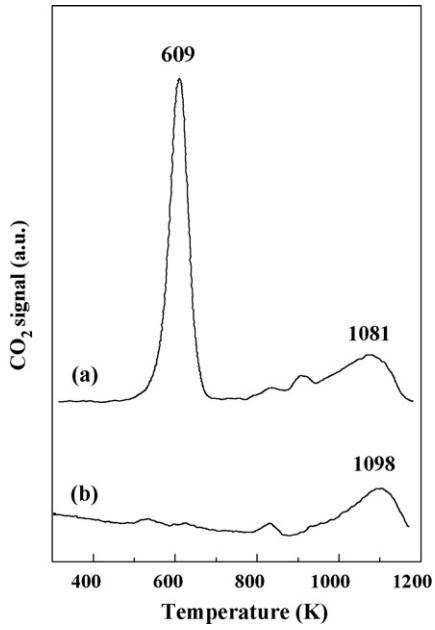

Fig. 9. TPO profiles of (a) Pt/CeO_2 and (b) $PtSn_4/CeO_2$ catalysts obtained after SR reaction.

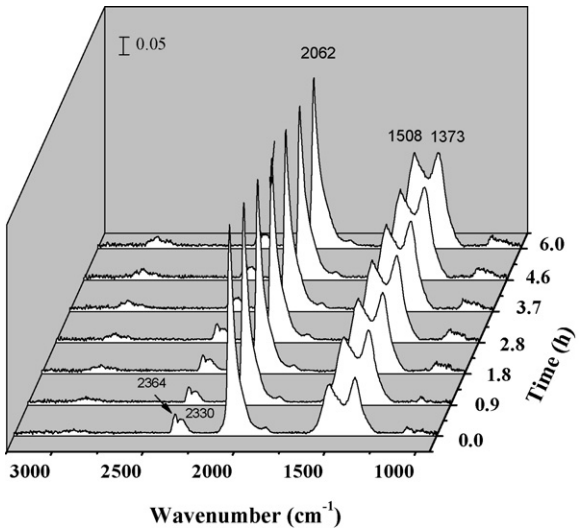

Fig. 10. DRIFTS spectra of Pt/CeO_2 obtained during SR reaction at 773 K under a steady flow of the ethanol + water mixture.

during SR at 773 K for the sample containing the higher tin loading.

According to the TPD and DRIFTS results, the reaction mechanism is similar over all catalysts studied. However, the presence of tin inhibited some reaction pathways. Ethanol adsorbs in a dissociative manner to form ethoxy species and may follow two distinct pathways: (i) decomposition and production of CO, CH_4 and H_2; or (ii) dehydrogenation to acetaldehyde and acetyl species. On PtSn-based catalysts the route involving the decomposition of ethoxy species is inhibited. Thus, the dehydrogenated species either desorb as acetaldehyde or undergo oxidation to acetate species. The acetate species can be decomposed to methane and CO or oxidized to carbonate species that are further decomposed to CO_2. The decomposition reactions are facilitated over Pt/CeO_2 catalyst and result in high selectivities to hydrogen, methane and CO during SR. On the other hand, with PtSn-based catalysts, a fraction of the dehydrogenated species desorb as acetaldehyde, whereas another fraction is oxidized to carbonate via acetate species.

As discussed above, the deactivation of Pt-based catalysts during SR should be attributed to deposition of carbonaceous residue. In order to evaluate the effect of Sn addition on the nature of the carbon formed during the reaction, TPO experiments were carried out after SR over Pt/CeO_2 and $PtSn_4/CeO_2$ catalysts.

3.3. Catalyst deactivation

3.3.1. TPO analysis after SR

The TPO profile of Pt/CeO_2 exhibited two peaks at 609 and 1081 K corresponding to CO_2 formation (Fig. 9). The peak at low temperature is much more prominent than the one at high temperature. The amount of carbon deposited corresponding to the peak at 609 K was higher than that related to the peak at 1081 K (Table 2). In the case of $PtSn_4/CeO_2$ catalyst, only one CO_2 production peak was detected at high temperature (1098 K) and the amount of carbon deposited was lower than that observed for the Pt/CeO_2 catalyst (Table 2). In addition, the peak at high temperature is much more prominent than the one at low temperature.

Noronha et al. [39] studied the nature of carbon formed over supported platinum catalysts during dry reforming of CH_4 by TPO experiments performed after reaction. They detected two different oxidation regions, which were assigned to different locations of carbon species on the catalyst surface. The peak in the low-temperature region was attributed to carbon located in close proximity to the metal particles, whereas the one at high temperature region was assigned to carbon on the support. Therefore, in this work, the peaks at 609 and 1081–1098 K could be attributed to carbon formed near the metal particle and the carbon deposited on the support, respectively. Moreover, the results show that the presence of Sn suppresses the formation of carbon on the catalyst surface, mainly over metallic sites. This result can explain the lower deactivation rate observed when tin was added to the catalyst.

In order to determine the nature of the intermediate species formed over the catalyst surface during reaction at 773 K on Pt/CeO_2, $PtSn/CeO_2$ and $PtSn_4/CeO_2$, DRIFTS spectra were recorded during 6 h under a steady flow of the ethanol + water mixture.

3.3.2. DRIFTS spectra obtained during SR reaction under a steady flow of the ethanol + water mixture

The DRIFTS spectra obtained at the beginning of the reaction for Pt/CeO_2, $PtSn/CeO_2$ and $PtSn_4/CeO_2$ catalysts (Figs. 10–12) were similar to the ones observed at 773 K in Figs. 6–8. The presence of ν(OCO) bands at 1300–1600 cm^{-1} and the absence of the C–H stretching bands (2970–2880 cm^{-1}) indicate that the carbonate species are the main species formed over all samples studied. The band related to gas phase CO_2 (~2350 cm^{-1}) was observed over all the catalysts studied. On the other hand, the band associated with adsorbed CO over Pt was only detected over Pt/CeO_2 (2062 cm^{-1}) and $PtSn/CeO_2$ (2040 cm^{-1}).

During the reaction, significant changes were noted in the DRIFTS spectra of Pt/CeO_2 (Fig. 10) and $PtSn/CeO_2$ (Fig. 11) catalysts. For the Pt/CeO_2 catalyst, the intensities of bands at 1300–1600 cm^{-1} and 2970–2880 cm^{-1} (i.e., C–H stretching) increased with TOS, indicating that the surface population of acetate species increased. Furthermore, an increase in the inten-

Table 2
Amount of carbon formed during the TPO experiments performed after SR over Pt/CeO_2 and $PtSn_4/CeO_2$ catalysts.

Catalyst	Pt/CeO_2		$PtSn_4/CeO_2$
Temperature (K)	609	1081	1098
Carbon formed (mg_{carbon}/g_{cat})	5.9	3.1	1.5
Total carbon	9.0		1.5

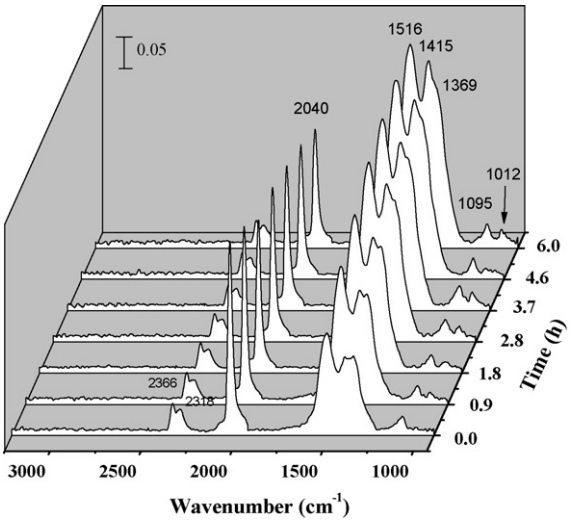

Fig. 11. DRIFTS spectra of $PtSn/CeO_2$ obtained during SR reaction at 773 K under a steady flow of the ethanol + water mixture.

sity of the bands assigned to acetate species was accompanied by a decrease in those corresponding to adsorbed CO over Pt. This result suggests that the rate of surface acetate decomposition decreased during the reaction, leading to an increasing steady-state inventory on the catalyst surface. de Lima et al. [12] also reported similar findings for DRIFTS experiments carried out over $Pt/CeZrO_2$ catalysts under SR reaction conditions during 6 h TOS at 773 K. They proposed that the decomposition of acetate species is facilitated by the Pt–support interface, producing CH_x species and CO. Therefore, the decrease in the intensity of the adsorbed CO band was attributed to a loss in Pt active sites due to the accumulation of CH_x species at the Pt–support interface, resulting in catalyst deactivation. Then, in our work, the increasing coverage of acetate species on the catalyst surface with TOS indicates that the turnover rate for acetate decomposition decreases (i.e., acetate steady-state coverage increases with TOS) due to an accumulation of CH_x species at the Pt–oxide interface.

In the case of $PtSn/CeO_2$ catalyst, the bands around 1300–1600 cm^{-1} significantly increased with TOS. However, the bands in the wavenumber region between 2970 and 2880 cm^{-1} were not detected during 6 h TOS. This indicates that this sample contains mainly carbonate species that increased with TOS.

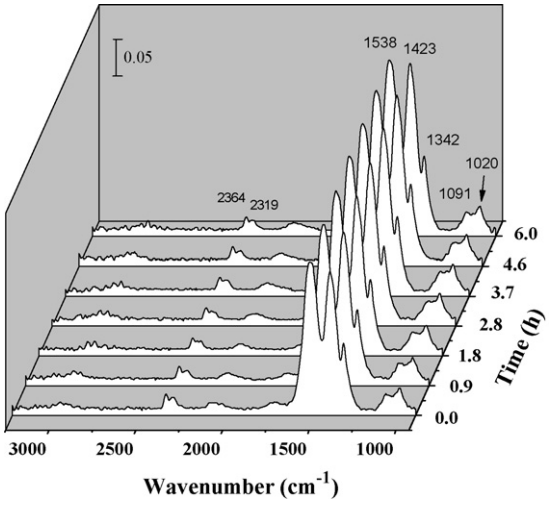

Fig. 12. DRIFTS spectra of $PtSn_4/CeO_2$, obtained during SR reaction at 773 K under a steady flow of the ethanol + water mixture.

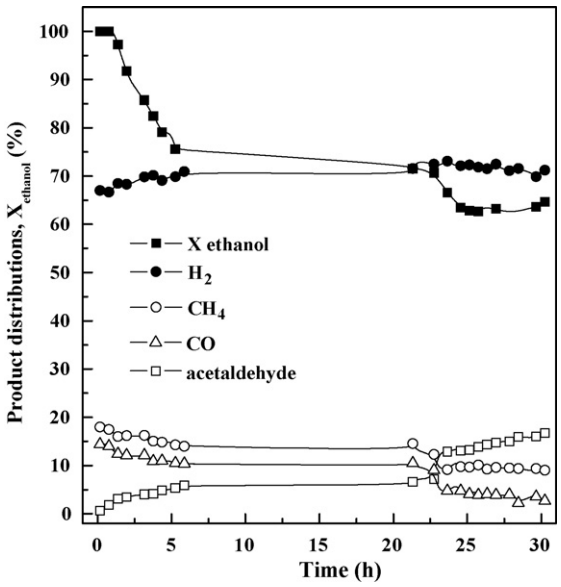

Fig. 13. Ethanol conversion ($X_{ethanol}$) and product distributions versus TOS obtained for SR in the presence of CO_2 over Pt/CeO_2. *Reaction conditions*: mass of catalyst = 20 mg; $T_{reaction}$ = 773 K; H_2O/ethanol molar ratio = 10.0; CO_2/ethanol molar ratio = 4.0; residence time = 0.02 g s/mL.

In addition, the intensity of the bands related to adsorbed CO decreased during SR, as observed over Pt/CeO_2 catalyst. A slight decrease in CO_2 formation was also noted. This result suggests that the rate of decomposition of carbon species decreased, leading to the accumulation of CH_x species on the catalyst surface and the desorption of acetaldehyde during the reaction.

On the other hand, the spectra for $PtSn_4/CeO_2$ exhibited only the bands attributed to carbonate species (1342, 1423 and 1538 cm^{-1}) and gas phase CO_2 (Fig. 12). Contrary to the results observed for Pt/CeO_2 and $PtSn/CeO_2$ catalysts, only a slight increase in the intensity of the bands assigned to carbonate species was detected for $PtSn_4/CeO_2$ during SR at 773 K.

Taking into account the reaction mechanism proposed by the results obtained from analysis of TPD and *in situ* DRIFTS, the decomposition of dehydrogenated species and the steam-assisted forward demethanation of acetate species, which generates the CH_x species, were inhibited by the presence of the Pt–Sn interaction. Therefore, the rate of accumulation of CH_x species at the metal–support interface should be lower over PtSn-based catalysts, reducing the deactivation rate of the catalyst. Unfortunately, the improved stability with PtSn is at the expense of poorer catalyst selectivity (e.g., higher acetaldehyde) relative to Pt alone.

3.4. The effect of the addition of CO_2 to the feed

3.4.1. SR in the presence of CO_2 over Pt/CeO_2

Fig. 13 shows the ethanol conversion and product distributions as a function of TOS for Pt/CeO_2 catalyst during SR at 773 K, using a H_2O/ethanol of 10.0 and a CO_2/ethanol molar ratio of 4.0. After a period of deactivation, the catalyst remained stable at a high conversion level (~64%). Hydrogen is the main product formed, although small amounts of CH_4, CO and acetaldehyde were also detected.

Comparing these results with those obtained without CO_2 in the feed (Fig. 2a), it is clear that the addition of CO_2 significantly improved the stability of the catalyst and favored CO and acetaldehyde formation. Three phenomena should be considered which can lead to a higher stability of the catalyst in the presence of CO_2: (1) dry reforming of CH_4 formed by the decomposition of carbon

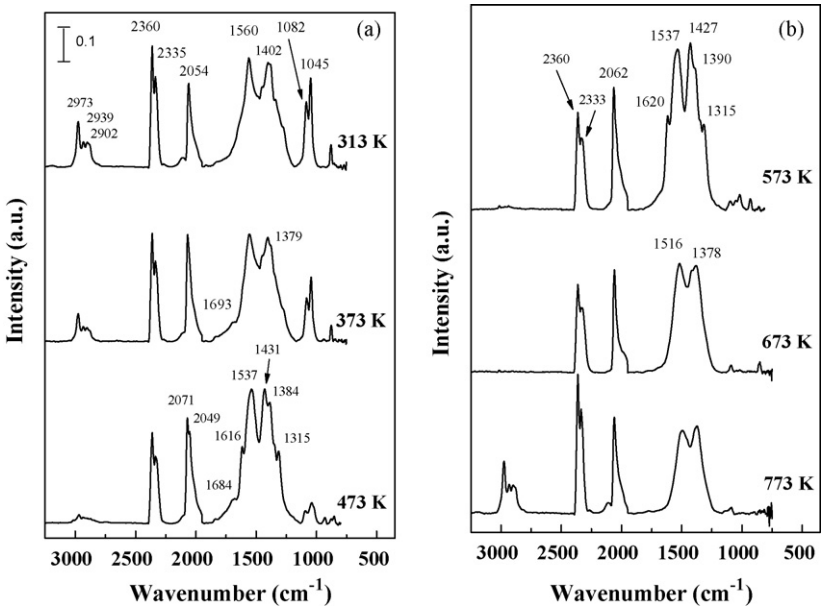

Fig. 14. DRIFTS spectra obtained on Pt/CeO_2 catalyst at different temperatures and under the reaction mixture containing ethanol, water and CO_2 (H_2O/ethanol molar ratio = 2.0; CO_2/ethanol molar ratio = 4.0).

species, reducing the accumulation of CH_x species at the Pt–support interface; (2) a shift in the equilibrium of the Boudouard reaction (reaction (3)) to the reactant side that leads to a reduction in the formation of carbon and an increase in the formation of CO; or (3) CO_2 competition with ethanol for the same adsorption sites, reducing the rate of the decomposition of carbon species, which directly impacts the rate of CH_x species formation.

In order to evaluate the activity of Pt/CeO_2 catalyst during dry reforming of CH_4, the reaction between CH_4 and CO_2 was performed at the same temperature used for SR. The results (not presented) showed that Pt/CeO_2 exhibited a very low CH_4 conversion, which suggests that this reaction does not contribute significantly to the higher stability of the catalyst during SR reaction at 773 K in the presence of CO_2.

Galetti et al. [40] reported that the reverse of the Boudouard reaction becomes significant at 973 K, increasing the catalyst resistance to deactivation. Therefore, the contribution of the reverse of Boudouard reaction to the removal of carbon through the addition of CO_2 to the feed should not be important.

To probe the kinetic influence of co-feeding CO_2 during SR, DRIFTS spectra for Pt/CeO_2 catalyst were recorded at different temperatures under a mixture of ethanol + water + CO_2.

3.4.2. *DRIFTS over Pt/CeO_2 during SR with CO_2 co-feeding*

Fig. 14 shows the DRIFTS spectra at different temperatures under the ethanol + water + CO_2 mixture. The assignments of the IR bands were similar to those obtained under the ethanol/water feed. However, in this case, the intensities of the bands corresponding to carbonate species and CO_2 were much higher. In addition, these bands are present at all temperatures studied. This result indicates that CO_2 competes with ethanol for the same adsorption sites.

From room temperature to 573 K, the intensities of the bands assigned to ethoxy species decreased whereas an increase in the intensities of the bands corresponding to acetate and carbonate species was identified. Slight increases in the intensities of bands related to adsorbed CO and CO_2 were also observed. Furthermore, the appearance of a band around 1684–1693 cm^{-1} at 373 and 473 K was observed, which is likely attributed to acetaldehyde [12,29]. At 573 K, the absence of the bands in the region between 2880 and 2970 cm^{-1} suggest that carbonate species are the main species on the catalyst surface. Increasing the temperature to 773 K decreased the intensities of all bands but they are still present.

Comparing the results with the spectrum obtained during feeding of ethanol and water alone (Fig. 6), significant differences in the relative band intensities were observed. The ratio between the intensities of adsorbed CO/ethoxy species and adsorbed CO/acetate species significantly decreased in the presence of co-fed CO_2 (adsorbed CO refers to ν(CO) of CO adsorbed on Pt particles). This result suggests the rate of decomposition of carbon species was reduced by the presence of CO_2. Since CH_x species are formed by the decomposition reactions, the accumulation of these species over the catalyst surface should be lower when CO_2 is added to the feed. This could explain the higher stability of Pt/CeO_2 catalyst in the presence of CO_2. In addition, the ratio between the intensities of carbonate/ethoxy species strongly increased in the case of co-feeding CO_2. This result indicates that CO_2 and ethanol compete for the same adsorption sites, which may decrease the ethanol reaction rate.

4. Conclusions

Differences in activity and selectivities were observed between high and low surface area unpromoted ceria materials during ethanol steam reforming, confirming that the oxide carrier is active. However, the selectivities to ethylene and acetaldehyde were high over the low and high surface area materials, respectively. Improved initial yields of hydrogen were obtained by adding Pt to ceria, and in agreement with this, initial ethylene and acetaldehyde selectivities were correspondingly much lower. TPD and DRIFTS mechanistic experiments confirmed that the role of Pt is to assist in dehydrogenating and demethanating adsorbed intermediates on the surface. Ethoxy species are dehydrogenated and acetate is produced by the addition of support-bound hydroxyl species to the dehydrogenated intermediates. The Pt not only assists in dehydrogenating ethoxy species (i.e., hydrogen transfer reactions), but also in the forward steam-assisted acetate demethanation reaction. Increasing the steam content also improved catalyst stability, but

the effect was only short-term. In all cases, an increase in acetaldehyde selectivity with TOS was observed and is indicative of an increasing inhibition of the ability of Pt to operate on the intermediates at the Pt–ceria interface. TPO experiments revealed that the Pt function was suppressed by carbon formation.

To improve stability, two approaches were undertaken. First Sn was alloyed with Pt in an attempt to suppress the carbon formation reaction. Ethanol hydrogenolysis, an ensemble sensitive reaction, confirmed alloy formation. Unfortunately, although the catalyst with high Sn content exhibited greater stability, the acetaldehyde selectivity was prohibitive. As confirmed by DRIFTS experiments, Sn tended to inhibit the ability Pt to facilitate forward acetate decomposition. However, the second approach utilized, that of CO_2 co-feeding, proved to be more effective in promoting long-term stability in reaction tests. DRIFTS experiments strongly suggest that CO_2 competes with ethanol for adsorption sites, thereby suppressing the rate of formation of coke precursors.

Acknowledgements

This work received financial support of CTENERG/FINEP-01.04.0525.00. CAER acknowledges the Commonwealth of Kentucky for financial support.

References

[1] P.R. de la Piscina, N. Homs, Chem. Soc. Rev. 37 (2008) 2459.
[2] P.D. Vaidya, A.E. Rodrigues, Ind. Eng. Chem. Res. 45 (2006) 6614.
[3] A. Haryanto, S. Fernando, N. Murali, S. Adhikari, Energy Fuels 19 (2005) 2098.
[4] H. Song, L. Zhang, R.B. Watson, D. Braden, U.S. Ozkan, Catal. Today 129 (2007) 346.
[5] R.M. Navarro, M.C. Alvarez-Galvan, M.C. Sanchez-Sanchez, F. Rosa, J.L.G. Fierro, Appl. Catal. B 55 (2004) 223.
[6] M. Veronica, B. Graciela, A. Norma, L. Miguel, Chem. Eng. J. 138 (2008) 602.
[7] A.N. Fatsikostas, X.E. Verykios, J. Catal. 225 (2004) 439.
[8] A. Erdohelyi, J. Raskó, T. Kecskés, M. Tóth, M. Dömök, K. Baán, Catal. Today 116 (2006) 367.
[9] V. Fierro, V. Klouz, O. Akdim, C. Mirodatos, Catal. Today 75 (2002) 141.
[10] M. Mavrikakis, M.A. Barteau, J. Mol. Catal. 131 (1998) 135.
[11] A. Yee, S.J. Morrison, H. Idriss, J. Catal. 186 (1999) 279.
[12] S.M. de Lima, A.M. Silva, U.M. Graham, G. Jacobs, B.H. Davis, L.V. Mattos, F.B. Noronha, Appl. Catal. A 352 (2009) 95.
[13] M. Domok, M. Tóth, J. Raskó, A. Erdohelyi, Appl. Catal. B 69 (2007) 262.
[14] M.A. Goula, S.K. Kontou, P.E. Tsiakaras, Appl. Catal. B 49 (2004) 135.
[15] H. Roh, A. Platon, Y. Wang, D.L. King, Catal. Lett. 110 (2006) 1.
[16] A. Platon, H.S. Roh, D.L. King, Y. Wang, Top. Catal. 46 (2007) 374.
[17] D.K. Liguras, D.I. Kondarides, X.E. Verykios, Appl. Catal. B 43 (2003) 345.
[18] W. Cai, F. Wanga, E. Zhan, A.C. Van Veen, C. Mirodatos, W. Shen, J. Catal. 257 (2008) 96.
[19] F. Romero-Sarria, J.C. Vargas, A. Roger, A. Kiennemann, Catal. Today 133 (2008) 149.
[20] J.C. Vargas, S. Libs, A.C. Roger, A. Kiennemann, Catal. Today 107 (2005) 417.
[21] J.M. Guil, N. Homs, J. Llorca, P.R. de la Piscina, J. Phys. Chem. B 109 (2005) 10813.
[22] A.E. Galetti, M.F. Gomez, L.A. Arrua, A.J. Marchi, M.C. Abello, Catal. Commun. 9 (2008) 1201.
[23] H. Wang, Y. Liu, L. Wang, Y.N. Qin, Chem. Eng. J. 145 (2008) 25.
[24] V. Klouz, V. Fierro, P. Denton, H. Katz, J.P. Lisse, S. Bouvot-Mauduit, C. Mirodatos, J. Power Sources 105 (2002) 26.
[25] A.N. Fatsikostas, D.I. Kondarides, X.E. Verykios, Chem. Commun. (2001) 851.
[26] F. Frusteri, S. Freni, V. Chiodo, S. Donato, G. Bonura, S. Cavallaro, Int. J. Hydrogen Energy 31 (2006) 2193.
[27] J. Llorca, N. Homs, J. Sales, P.R. de la Piscina, J. Catal. 209 (2002) 306.
[28] J. Kugai, V. Subramani, C. Song, M.H. Engelhard, Y.H. Chin, J. Catal. 238 (2006) 430.
[29] S.M. de Lima, I.O. da Cruz, G. Jacobs, B.H. Davis, L.V. Mattos, F.B. Noronha, J. Catal. 257 (2008) 96.
[30] H. Song, U.S. Ozkan, J. Catal. 261 (2009) 66.
[31] D.L. Trimm, Catal. Today 37 (1997) 233.
[32] M. Domok, K. Baan, T. Kecskes, A. Erdohelyi, Catal. Lett. 126 (2008) 49.
[33] J. Beltramini, D.L. Trimm, Appl. Catal. A 32 (1983) 149.
[34] S.M. de Lima, G. Jacobs, B.H. Davis, K.R. Souza, A.F.F. de Lima, L.G. Appel, L.V. Mattos, F.B. Noronha, in: Proc. Post-Symposium of the 14th International Congress on Catalysis – Catalysis for Hydrogen Energy Production and Utilization, 2008, p. 119.
[35] R. Alcala, J.W. Shabaker, G.W. Huber, M.A. Sanchez-Castillo, J.A. Dumesic, J. Phys. Chem. B 109 (2005) 2074.
[36] D.E. Resasco, G.L. Haller, J. Catal. 82 (1983) 279.
[37] L.V. Mattos, F.B. Noronha, J. Catal. 233 (2005) 453.
[38] C. Binet, M. Daturi, J.C. Lavalley, Catal. Today 50 (1999) 207.
[39] F.B. Noronha, E.C. Fendley, R.R. Soares, W.E. Alvarez, D.E. Resasco, Chem. Eng. J. 82 (2001) 21.
[40] A.E. Galetti, M.F. Gomez, L.A. Arrua, M.C. Abello, Appl. Catal. A 348 (2008) 94.